

Physically based molecular device model in a transient circuit simulator

Nikhil M. Kriplani^a, David P. Nackashi^a, Christian J. Amsinck^a, Neil H. Di Spigna^a,
Michael B. Steer^a, Paul D. Franzon^a, Ramon L. Rick^b, Gemma C. Solomon^c,
Jeffrey R. Reimers^{c,*}

^a Department of Electrical Engineering, North Carolina State University, Raleigh, NC 27695-7911, USA

^b Department of Electrical Engineering, University of Cooperative Education, 70174 Stuttgart, Germany Alcatel SEL, 70435 Stuttgart, Germany

^c School of Chemistry, The University of Sydney, NSW 2006, Australia

Received 14 September 2005; accepted 2 March 2006

Available online 9 March 2006

Abstract

Two efficient, physically based models for the real-time simulation of molecular device characteristics of single molecules are developed. These models assume that through-molecule tunnelling creates a steady-state Lorentzian distribution of excess electron density on the molecule and provides for smooth transitions for the electronic degrees of freedom between the tunnelling, molecular-excitation, and charge-hopping transport regimes. They are implemented in the *JREEDA*TM transient circuit simulator to allow for the full integration of nanoscopic molecular devices in standard packages that simulate entire devices including CMOS circuitry. Methods are presented to estimate the parameters used in the models via either direct experimental measurement or density-functional calculations. The models require 6–8 orders of magnitude less computer time than do full a priori simulations of the properties of molecular components. Consequently, molecular components can be efficiently implemented in circuit simulators. The molecular-component models are tested by comparison with experimental results reported for 1,4-benzenedithiol.

© 2006 Elsevier B.V. All rights reserved.

Keywords: Molecular electronics; Circuit simulator; Density-functional theory, 1,4-Benzenedithiol; Single-molecule conductivity

1. Introduction

Molecular electronics is emerging as a potential alternative to conventional semiconductor technology with advantages in terms of functional density and integration. The technology is based on the operation of single molecules or groups of molecules as device components and has the potential to overcome the scalability barrier faced by current semiconductor technology. Its origins stem from the Marcus–Hush electron-transfer theory [1–3], as envisaged in the seminal paper by Aviram and Ratner describing molecular rectifiers [4]. Recent research has focused on the elucidation of the basic properties of molecular components through both experimental design of test beds as well as through theoretical modelling. Now, there is consider-

able interest in the overall system design of potential devices embodying molecular components. Early commercial applications are expected to embody hybrid technologies in which standard CMOS electronics with its associated lithography techniques is used to build connections from the nanoscopic world to the macroscopic world. Such systems will have close coupling between molecular and semiconductor electronics. A key contributor to the advance of semiconductor technology has been the availability of circuit simulators that can predict the operating characteristics of integrated circuits containing perhaps over 10^8 individual components. Hence the practical development of hybrid electronics containing molecular components requires the development of a circuit-element simulator that uses compact models of the molecular components. Other required properties are accuracy and adaptability so that large numbers of different molecular components may be treated.

* Corresponding author.

E-mail address: j.reimers@chem.usyd.edu.au (J.R. Reimers).

First-principles quantum simulations of the current passing through a molecular device offer both accuracy and adaptability; these are typically performed using density-functional theory (DFT) [5–10]. As the chemical interactions that control the nature of molecule–metal and molecule–semiconductor interfaces are usually long range, the inclusion of a large number of electrode atoms in these calculations is unfortunately essential [11]. As a result, first-principles simulations are currently 6–8 orders of magnitude too slow to be useful in circuit simulators, and enhancements such as linear scaling algorithms or the use of faster approaches such as INDO [12] are not capable of delivering the required performance.

Alternatively, the use of fully empirical descriptions of the current as a function of voltage applied across a two-terminal device can lead to very efficient simulations. Approaches of this type have been quite successful [13–19] in modelling entire integrated-circuit systems containing nanotubes, DNA wires, and molecular conductors. Features that can be modelled in this way include basic rectification as well as hysteresis loops in which the current is a function of the past voltages as well as the instantaneous voltage, without requiring either excessive memory storage or excessive evaluation times, thus allowing say negative differential resistance to be modelled. Indeed, any two-terminal molecular component could be implemented using an empirical approach. Empirical models are designed a system at a time, however, requiring in their development experimental data for the specific system of interest under conditions similar to that found in the device. Unfortunately, a very large amount of experimental data are required to empirically characterize three-terminal and more complicated devices, making the generation of models tedious. In addition, models are difficult to modify in order to incorporate small changes to the system made, for example, by chemical substitutions to the molecule.

There is thus the increasing need for the development of an intermediary approach between fully first-principles simulations and fully empirical ones. An intermediate approach is to use a physically based model containing a small number of observable and/or calculable physical parameters that is capable of determining the properties of complex molecular components. Such a model requires adaptation only for each particular type of molecular component, not for each possible example of that type that could be produced say by chemical substitution or combinatorial synthesis, and the precise features that must be included within it need only be determined in the context of the required accuracy. Herein we determine a basic approach to underlie models of this type for arbitrary molecular devices and model a simple two-terminal molecular-wire type component.

The molecular component model developed is implemented in the circuit simulator *f*REEDA™ [20]. This simulator uses a universal modelling technology and object-oriented programming principles that enable the same piece of computer code to be used with any analysis

type. Device models in *f*REEDA™ have global convergence properties and use a state-variable approach that enables smooth model development as it is sufficiently general to allow for the unusual properties that molecular devices may possess. Alternative model implementation approaches, for example, those utilized in the SPICE [21] circuit simulator, are cumbersome as they require the introduction of artificial voltage-like and current-like quantities for the description of molecular components [22]. Another very useful feature of *f*REEDA™ is implementation of automatic differentiation [23] making explicit evaluation of derivatives unnecessary.

Section 2 describes the basic physical model for transport through and into a many-level molecule. This allows solutions to be generated using the single-level tunnelling formalism developed by Datta et al. [24,25]. Two different implementations are presented called Model #1 and Model #2, these varying in physical completeness and computational efficiency. The appropriateness of these models is demonstrated first in Section 3 where known analytical expressions for the current passing through a molecular wire composed of a string of atoms are reproduced analytically. Section 4 discusses the implementation of the models in the *f*REEDA™ circuit-simulator environment, including timing information. Section 5 discusses the physical significance of the parameters used in the model. The parameters may be determined from either experimental data or from first-principles calculations, with DFT being used in the section to determine the parameters for a sample 1,4-benzenedithiol molecular wire. In Section 6, results from *f*REEDA™ simulations are compared to experimental data measured in molecular junction experiments [26] for chemisorbed 1,4-benzenedithiol.

2. Physical device models

Determining the electrical behavior of a molecule requires that the molecule be positioned between contact electrodes. Exact positioning of the molecules is not easy considering that the length of the typical molecules is just a few nanometers, smaller dimensions than can be controlled using modern photolithography. Currently, the attachment of molecules to metallic electrodes is achieved typically by random deposition of molecules on the electrode surface out of a molecule-rich solution. This results in a densely packed layer of molecules or a self-assembled monolayer (SAM) and the molecule–metal bond often involves a sulfur atom, either as a chemisorbed thiol or a physisorbed disulfide. One way of measuring electrical conductance characteristics of a small number of molecules is to build a nanopore [26] (with a diameter of a few nanometers), filled with a SAM typically containing a few hundred to a thousand molecules sandwiched between two electrodes. Regardless of the method of preparation, a rough schematic view of the structure is usually evoked involving idealized flat contact surfaces and unmoving molecules, of the kind sketched in Fig. 1. Measurements on molecular

conductors have been performed with nanopores [27], between crossed wires [28–30], between nanocluster dimers [31], as well as by using a scanning tunneling microscope (STM) [32]; a review of early experimental work has been given by Reed [33]. However, even for thiol monolayers on flat gold surfaces [34–37], the interface structure is not fully understood with many different structures possible. First-principles calculations require the atomic coordinates of the interface, but in experimental devices many and varied configurations are typically involved. In a practical circuit simulator, a means is required to overcome this limitation. We develop a physically based model that captures the key quantum mechanical features whilst allowing for some degree of empiricism to account for the average structural properties that affect quantitative performance.

Datta et al. [24,25] have described two physically based models for the transport of electrons between reservoirs associated with the contacts through a sandwiched molecule. The chemical potentials of the electrons (“electrochemical potentials”) in the contacts are given by

$$\mu_1 = E_F + \eta eV \quad (1)$$

for Contact 1 and

$$\mu_2 = E_F - (1 - \eta)eV \quad (2)$$

for Contact 2. Here E_F is the Fermi energy of the contacts at zero bias, e is the magnitude of the charge on the electron, $0 < \eta < 1$ is the voltage division factor between the

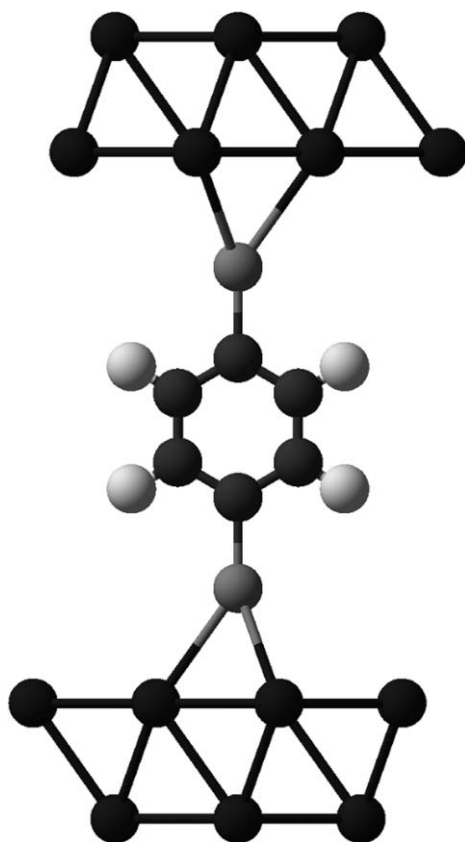


Fig. 1. Sketch of a conceptualized interface between two contact electrodes and a chemisorbed 1,4-benzenedithiol molecule.

two electrodes and V is the potential difference (bias) between Contact 2 and Contact 1. The molecule is chemisorbed onto each of the metallic contacts so there is a strong coupling between the contacts and the molecule. This allows for charge transfer to take place, a phenomenon that is modulated by the applied bias, and for molecular energy-level broadening. The relative coupling strengths of the two contacts is accounted for by separating the total broadening Γ into contributions Γ_1 and Γ_2 from each contact, where $\Gamma = \Gamma_1 + \Gamma_2$. The magnitude of the contact-molecule-contact electron transport is controlled by both this broadening and the orbital charging energy (i.e., the energy required to oxidize or reduce the molecule in situ). In the simplest possible quantum description of the processes happening on the molecule [38], the orbital charging energy is expressed as a function of two parameters, the two-electron interaction energy U_0 and the equilibrium molecular-orbital energy ϵ_0 . Generally, if $\Gamma \ll U_0 \ll |E_F - \epsilon_0|$, the transport is said to be in the Coulomb blockade region. Here charge is only transferred to the molecule at a critical voltage, and the amount transferred is integral; current can then be passed through a long molecule in a stepwise fashion known as charge hopping. If these limits do not hold, then tunnelling becomes important with significant current and steady-state charge transfer at voltages less than that required for energy-level resonance. However, this treatment is simplistic in that it ignores the geometrical relaxation processes that accompany charge transfer, the reorganization energy contribution that dominates Marcus–Hush electron-transfer processes [1–3] including soliton transport and charge hopping. Indeed, it is argued by Larsson in this Special Issue [39] that the reorganization energy is generally more important than the two-electron interaction energy U_0 ; its manifestations are known to be important in low-temperature devices for which inelastic scattering phenomena become important [40,41]. The approach taken herein accounts for molecular relaxation by treating U_0 not simply as a two-electron interaction energy but rather as a parameter that specifies the equilibrium molecular reduction or oxidation potential. For molecular orbitals that are unoccupied this generalized U_0 specifies the reduction potential so that charge transport occurs via electron transfer into the molecule, whereas for doubly occupied molecular orbitals it specifies the oxidation potential so that charge transport occurs via hole transfer into the molecule. These processes are directly akin to intramolecular and intermolecular electron-transfer and hole-transfer processes except that the system occurs in a non-equilibrium steady-state induced by the applied voltage.

The application of voltage to the contacts (electron reservoirs) causes them to have different electrochemical potentials, see Eqs. (1) and (2). Each contact then transfers charge by electron or hole tunnelling into the molecule in an attempt to bring the molecule into equilibrium with itself, thus establishing steady-state current flow. Molecules have many energy levels that interact with the electrodes

and with each other, and in first-principles calculations a single solution is obtained that simultaneously accounts for all of these features. We introduce a key assumption that allows for extremely fast computations: the interaction of the contacts with an orbital is taken to be independent of the interactions with other orbitals, writing the total molecular charge as the sum of the individual orbital charges. This is nearly tantamount to assuming that each molecular energy level behaves as an independent component, with the net conduction represented as the component sum. It allows the single-level conduction models developed by Datta et al. [24,25] to be directly applied. Simultaneous electron and hole transport through the molecule is allowed and results in the promotion of the molecule to high-energy electronic states, with the excited-state energies being given by the zeroth-order approximation as molecular-orbital energy differences. Away from the contacts, each orbital must be either fully occupied or fully unoccupied, but in assembled devices the contact with the higher electrochemical potential pushes electrons into the molecule while the contact with the lower one pulls electrons out, each electrode trying to achieve local equilibrium across its junction. A steady-state is reached when the tunnelling currents at each interface are equal, and the net charge transferred to the molecule adjusts to achieve this scenario.

The number of electrons in a single molecular orbital required to establish equilibrium with Contact 1 is

$$N_1 = 2f(\epsilon_0, \mu_1), \quad (3)$$

where

$$f(\epsilon_0, \mu) = \frac{1}{1 + \exp\left(\frac{\epsilon_0 - \mu}{kT}\right)} \quad (4)$$

is the Fermi–Dirac distribution, and similarly for Contact 2

$$N_2 = 2f(\epsilon_0, \mu_2). \quad (5)$$

If N is the actual instantaneous number of electrons in the molecular orbital, the electrical current from contact to molecule is proportional to the perturbations $N - N_1$ relative to Contact 1 and $N - N_2$ relative to Contact 2, as well as to the corresponding carrier exchange rates $e\Gamma_1/\hbar$ and $e\Gamma_2/\hbar$ between the molecule and Contacts 1 and 2 respectively. In the steady-state these rates must be equal and hence

$$I = -\frac{e\Gamma_1}{\hbar}(N - N_1) = \frac{e\Gamma_2}{\hbar}(N - N_2) \quad (6)$$

from which immediately follows [24,25] the steady-state tunnelling condition

$$N = 2 \frac{\Gamma_1 f(\epsilon_0, \mu_1) + \Gamma_2 f(\epsilon_0, \mu_2)}{\Gamma_1 + \Gamma_2} \quad (7)$$

so that

$$I = \frac{2e}{\hbar} \frac{\Gamma_1 \Gamma_2}{\Gamma_1 + \Gamma_2} (f(\epsilon_0, \mu_1) - f(\epsilon_0, \mu_2)). \quad (8)$$

This single-energy-level model serves to illustrate the mechanism of current flow in this contact-molecule-contact

structure. The current flow arises from the difference in the energy levels of the contacts. In the formulation presented so far, the energy level of the molecule is assumed constant. However, due to chemisorption and the applied bias, the number of carriers in the molecule changes from its isolated-molecule value, as specified by Eq. (7). The molecule therefore acquires a partial charge which is constant in time for a steady-state current and bias. Due to charging, the energy level shifts from its isolated-molecule value ϵ_0 to a new value ϵ . If there are N electrons in the molecular orbital, then the energy level shifts by an amount U_{SCF} proportional to the excess charge given as

$$U_{\text{SCF}} = U_0(N - N_0), \quad (9)$$

where N_0 represents the number of carriers in the isolated molecule: $N_0 = 2$ for an occupied orbital and 0 for an unoccupied one. Due to this charging, the energy level of the electron floats higher (unoccupied orbital) or lower (occupied orbital) by

$$\epsilon = \epsilon_0 + U_{\text{SCF}}. \quad (10)$$

If more than one energy level is interacting with the electrodes, then to a first approximation all energy levels change by an amount equal to the sum of all the individual U_{SCF} values. Through this modification, the equations for a single interacting level are easily enhanced to describe multiple interacting levels.

The steady-state electron transfer (Eq. (7)) and current (Eq. (8)) are functions of the energy level ϵ and hence energy-level broadening affects the current flow. This broadening may be expressed [24,25] in terms of a density of states, assumed to be of Lorentzian form:

$$D(E) = \frac{1}{2\pi} \frac{\Gamma_1 + \Gamma_2}{(E - \epsilon)^2 + (\Gamma_1 + \Gamma_2)^2/4}. \quad (11)$$

By integrating N and I from Eqs. (7) and (8) over this Lorentzian density we obtain a modified version of the average number of electrons in the molecular orbital

$$N = 2 \int_{-\infty}^{\infty} D(E) \frac{\Gamma_1 f(E, \mu_1) + \Gamma_2 f(E, \mu_2)}{\Gamma_1 + \Gamma_2} dE \quad (12)$$

and the current

$$I = \frac{2e}{\hbar} \int_{-\infty}^{\infty} D(E) \frac{\Gamma_1 \Gamma_2}{\Gamma_1 + \Gamma_2} (f(E, \mu_1) - f(E, \mu_2)) dE. \quad (13)$$

Two alternative models for the molecular component have thus been derived: Eqs. (7) and (8) are called Model #1 whilst Eqs. (12) and (13) are called Model #2. Clearly, Model #1 is more computationally efficient than Model #2 but includes less of the basic physics of conduction.

3. Analytical solution of Model #1 for an atomic molecular wire

An interesting application of Model #1 is to tunnelling through an atomic wire consisting of a linear string of identical atoms. Its total conductivity may indeed be accurately

expressed as the sum of the conductivities through each individual orbital of the wire [42] and the simplest case is for conduction through just a single atom. At zero temperature for $\Gamma_1 = \Gamma_2$, and $U_0 = 0$, Eq. (8) evaluates to give

$$I = \frac{e\Gamma_1}{\pi\hbar} \left[\tan^{-1} \frac{(E_F - \epsilon_0 + eV/2)}{\Gamma_1} - \tan^{-1} \frac{(E_F - \epsilon_0 - eV/2)}{\Gamma_1} \right] \quad (14)$$

which is the same result obtained using more sophisticated Greens functions methods on the assumption of a constant electrode density of states [42]. For resonant conduction with $E_F = \epsilon_0$, this expression yields a zero-voltage resistance of $R_0 = 2e^2/h = 12.9 \text{ k}\Omega$, the quantum of resistance. As this result has been observed in gold atomic wires spanning gold electrodes [26,43–45], our conductance model reproduces an important practical conductance limit. Excellent results are thus expected for the circuit simulator if atomic molecular wires are present in a device.

4. Device model implementation in *fREEDA*TM

Models #1 and #2 have been implemented in *fREEDA*TM using the C++ language following algorithm development initially undertaken in FORTRAN. Both C++ implementation source files are less than 100 lines of code each, with the computational code being an order of magnitude smaller in size than that required for other electronic device simulators [22]. This demonstrates the suitability of the approach for use in real-time circuit simulators. However, for both models, a self-consistent procedure is required to determine the molecular energy level and its occupancy in a process that is akin to self-consistent loops in Hartree–Fock and DFT. In these a priori methods, obtaining self-consistent solutions for metal–molecule junctions is known to be a difficult procedure, and similar issues arise for the solution of our model equations. As a result, only small changes between iterations may be permitted so as to guarantee numerical stability, an effect that costs more computer time than would otherwise be expected.

Simulations have been performed on an IBM Thinkpad[®] using a Pentium[®] III 866 MHz processor to analyse the time consumption of Model #1, Model #2 using a parameter set that reduces the self-consistent iterations to a minimum (Model #2A), and Model #2 using the full physically most-consistent parameter set (Model #2B). The actual parameters used are given in Table 1 while the

Table 1
Parameter values for the molecular device models used in *fREEDA*TM from fits to the experimental data

Name	Model #1	Model #2A	Model #2B
Equilibrium energy level ϵ_0 (eV)	−4.967	−4.42	−4.52
Fermi levels $E_{F1} = E_{F2}$ (eV)	−5.1	−5.1	−5.1
Voltage division factor η	0.5	0.5	0.5
Broadening due to contacts $\Gamma_1 = \Gamma_2$ (eV)	0.0158	0.072	0.070
Orbital charging energy U_0 (eV)	1.262	0	1.03
Temperature T (K)	298	298	298

next section describes the source of these values. Model #1 is the most computationally efficient model, requiring less than 10 ms computer time to evaluate while Model #2B, the physically most-complete model, usually requires 1–10 s of computer time; while this amount is significant, it is acceptable for a circuit element of this complexity. Model #2A requires slightly more time than Model #1, and may constitute a compromise in practical calculations when maximum accuracy is not required.

5. Methods for determining the required molecular parameters: application to chemisorbed 1,4-benzenedithiol

As indicated in Table 1, for each system to be simulated, the following properties must be determined: the Fermi levels of the electrode contacts when in equilibrium, the voltage division factor η , the number of interacting molecular orbitals, and, for each such orbital, the couplings to the contacts Γ_1 and Γ_2 as well as the orbital charging energy U_0 . Of these, the Fermi energies of the isolated contacts are usually known experimentally, and from these the zero-voltage Fermi level E_F of the combined system can usually be estimated. Also, the voltage division factor can be taken as $\eta = 0.5$ if the two junctions are symmetric (note, however, that this factor can become very small in asymmetric applications such as STM imaging [46]). Hence only the molecular properties require effort to determine. We proceed by considering the specific example of 1,4-benzenedithiol chemisorbed between two gold contacts. As the electrodes are made of the same material, the Fermi level in equilibrium is simply the isolated-metal value $E_F = -5.1 \text{ eV}$.

Many experimental measurements have been performed on the gold–benzenedithiol–gold system from the original break-junction measurements of Reed et al. [27] to the recent sophisticated measurements of Xiao et al. [26]. Shown in Fig. 1 is the perceived device structure; the molecule depicted between the electrodes is not 1,4-benzenedithiol, however, as this species loses its thiol protons on chemisorption. The electronic structure of the dithiol and three possible alternatives for the chemisorbed species are shown in Fig. 2: the 1,4-benzenedithiyl biradical, 1,4-

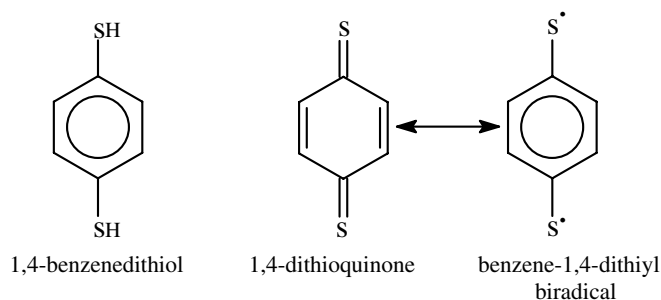


Fig. 2. 1,4-Benzenedithiol and possible representations of its chemical structure after loss of the thiol protons on chemisorption.

dithioquinone, and 1,4-benzenedithiolate. While chemisorbed thiols are often referred to in the literature as being “thiolates”, both experimental and theoretical evidence indicates that the binding has only ca. 20% thiolate character [34–37] and so only the two neutral species can be dominant contributors to the actual electronic structure. The neutral molecule has been isolated in the gas phase [47,48], although it is very reactive due to its propensity to polymerize via disulfide bond formation. As a result, it has not been thoroughly characterized, and it is unclear as to whether the open-shell (dithiyl) or closed-shell (dithioquinone) structure dominates. These subtleties in the electronic structure significantly influence through-molecule conductivity, and are determined as the *results* of a priori computations performed, for example, using DFT. Their nature, however, must be described as *input* to calculations using Model #1 or Model #2, and it is the understanding of these chemical issues that will dominate future physical-model-based circuit-simulator development. Indeed, these key questions are yet to be answered for this system, and their solution is outside the scope of this work. To complicate the process, the nature of the molecule is likely to alter as a function of solvation (both by the surrounding media and the presence of nearby contacts). Hence, while it is possible to use experimental data to determine the charging energies, the need to have these values in situ rather than in the gas phase, combined with the chemical reactivity of the adsorbate, precludes this possibility. We proceed making the simplest assumption that the gas-phase structure remains pertinent for the in situ environment, determining the orbital and charging energies from DFT simulations. This process is quite general and may be applied to all molecular systems in order to determine parameters for the circuit simulator. In the pertinent low-voltage region the couplings Γ_1 and Γ_2 act primarily to scale the computed current, and so values for these quantities are estimated fully empirically.

We consider only conduction through the highest-occupied molecular orbital (HOMO) or the lowest-unoccupied molecular orbital (LUMO), evaluating the structure and energies of the 1,4-benzenedithiyl biradical, its mono anion, its cation and its dianion (1,4-benzenedithiolate) using the GAUSSIAN03 [49] software package. The HOMO orbital has b_{3u} symmetry whilst the LUMO has b_{2g} . DFT is used in conjunction with the B3LYP [50] and PW91 [51] density functionals, computed using the 6–31+G** basis set [52]. To model the effects of the metal electrodes and surrounding liquid solvent, the calculated energies at the gas-phase optimized geometries are corrected using the COSMO dielectric continuum model for a nominal tetrahydrofuran solvent as well as through an image charge approach. In the image charge model, the interactions with the electrodes are included via

$$\Delta E = \sum_{ij} \frac{q_i q_j}{2r_{ij}}, \quad (15)$$

where q_i is the calculated atomic Mulliken charge for atom i in the gas phase and r_{ij} is the distance of this atom to each member of the infinite array of image charges j that result when a charge is sandwiched between two parallel conductors [54]. To calculate the distances r_{ij} , the molecule is placed vertically above the surface with the connecting sulfur atom 1.8 Å above the surface plane. This separation is obtained as an average of the separations for a likely chemisorption structures on a flat (111) gold surface [34]. All calculated energies are given in Table 2.

The parameters ϵ_0 and U_0 are closely related to those that appear in the Hubbard model [38] for molecular charging: ϵ_0 corresponds to the usual orbital energy whilst U_0 is half of the usual two-electron interaction term. Eq. (9) differs from the standard Hubbard expression as charging from the electrodes involves unpolarized partial electron transfer rather than transfer of whole polarized electrons. It also differs somewhat as the calculations allow for geometric relax-

Table 2

Estimates of the molecular parameters for chemisorbed 1,4-benzenedithiol represented as a weakly interacting 1,4-benzenedithiyl biradical, made using the B3LYP and PW91 density functionals; raw total energies E are in a.u. whilst the orbital properties ϵ_0 and U_0 are in eV

	B3LYP			PW91		
	Gas	SCRFA	Image charge ^b	Gas	SCRFA	Image charge ^b
$E(+2)$	–1026.5472	–1026.8124	–1026.5973	–1026.4388	–1026.7039	–1026.4856
$E(+1)$	–1027.0847	–1027.1573	–1027.0965	–1026.9607	–1027.0332	–1026.9692
$E(0)$	–1027.4010	–1027.4043	–1027.4334	–1027.2641	–1027.2673	–1027.2809
$E(-1)$	–1027.5098	–1027.5583	–1027.5687	–1027.3711	–1027.4191	–1027.4222
$E(-2)$	–1027.4240	–1027.7821	–1027.5984	–1027.3054	–1027.5273 ^c	–1027.5157
<i>HOMO</i>						
ϵ_0	–8.61	–6.72	–7.50	–8.26	–6.37	–7.53
U_0	3.01	1.33	1.73	2.98	1.30	1.73
<i>LUMO</i>						
ϵ_0	–2.96	–4.19	–4.43	–2.91	–4.13	–4.43
U_0	2.34	0.95	1.01	2.35	0.59 ^c	1.04

^a For tetrahydrofuran solvent, dielectric constant = 7.58.

^b Obtained non-self consistently using the gas-phase Mulliken charges for a vertically oriented molecule between two gold surfaces with a S to surface distance of 1.8 Å (a typical distance for likely adsorbate structures, see [34]).

^c Estimated from the solvation energy using the 6-31G basis set.

ation of the molecule and hence convolve electron-phonon interaction terms in with the electronic interaction term. While in highly accurate calculations, explicit treatment of these terms in accordance with standard Marcus–Hush theory is essential [39], implicit treatments are much simpler and at this stage appear to be generally useful. The required parameters are determined from the calculated molecular energies $E(n)$ for net molecular charge n as

$$\epsilon_0(\text{HOMO}) = E(0) - E(1), \quad (16)$$

$$\epsilon_0(\text{LUMO}) = E(-1) - E(0), \quad (17)$$

$$U_0(\text{HOMO}) = (E(2) - 2E(1) + E(0))/2, \quad (18)$$

$$U_0(\text{LUMO}) = (E(0) - 2E(-1) + E(-2))/2. \quad (19)$$

The deduced values of ϵ_0 and U_0 are also given in Table 2. The calculated gas-phase orbital energies are of the order -8 eV for the HOMO and -3 eV for the LUMO. These are far removed from the gold Fermi energy of $E_F = -5.1$ eV and suggest that rather large voltages are required in order to produce significant current flow. Solvation, however, significantly alters these orbital energies, with the dielectric solvation model moving both energies closer to E_F by ca. 1 eV. The image charge model has a similar effect indicating that these simplistic approaches do capture the key qualitative features of the physical aspects of the molecule-electrode interactions. As the experimentally observed conductivity (shown later in Fig. 3) is significant at low voltage, the absolute value of the difference between E_F and the dominant conduction-orbital energy must be small, for example, less than 1 eV. Calculations indicate that the HOMO lies far from this region while the LUMO falls within it. We hence deduce that the dominant conduction path is electron transport through the LUMO, and the

device is hence simulated using this orbital only. However, as discussed in the conclusions, improved models may lead to an alternate identification of the primary conduction orbital.

6. Simulating the conductivity of chemisorbed 1,4-benzenedithiol

The measurement of conductance through 1,4-benzenedithiol chemisorbed between gold surfaces has been reported most recently by Xiao et al. [26] by repeatedly creating and analyzing a large number of molecular junctions. The deduced current as a function of bias voltage is shown in Fig. 3. Calculated curves obtained using the *f*REEDA™ simulator for Model #1 and two variants of Model #2, named Model #2A and Model #2B, are also shown in this figure: The molecular parameters used in these simulations were fitted to the experimental data and are given in Table 1. Experimental data are only available in the low-voltage region, and all three models adequately fit the available data. However, at larger voltages the predicted curves differ significantly, indicating that, in principle, there are appreciable differences between these approaches.

The observed data has the appearance of a near-linear relation although some curvature is evident. It would thus appear that two parameters only are needed to describe it, yet Models #1 and #2 both contain 3 molecular parameters. The nature of Model #1 is such that it will, in general, provide large curvature in the low-voltage region, and so it actually yields a single sharply defined solution: $\epsilon_0 = -4.967$ eV, $\Gamma_1 = \Gamma_2 = 0.0158$ eV, and $U_0 = 1.262$ eV. This value of the orbital energy ϵ_0 is significantly different from the DFT estimates of -4.1 to -4.5 eV from Table 2 and is in fact very close to the contact Fermi energy $E_F = -5.1$ eV. Indeed, the neglect of energy-level broadening in Model #1 results in little conductivity until the voltage brings the molecular level to within ca. kT of a contact Fermi energy, hence effectively pinning the perceived molecular energy level to the Fermi energy. This is unphysical and indicates that this model is too simplistic to describe systems robustly.

The energy-level broadening included in Model #2 allows for significant conductivity near zero voltage, and we find that fitting its three parameters to the available experimental low-voltage data does present an underdetermined problem. Hence we use two sample solutions, Model #2 A in which we set $U_0 = 0$ and Model #2B in which it is set to a value typical of those predicted by DFT, 1.03 eV. In either case, realistic values of the orbital energy ϵ_0 emerge, -4.42 and -4.52 eV for Models #2A and #2B, respectively. Also, the fitted value of the couplings Γ are of the order of those evaluated using DFT and INDO computations on large supramolecular electrode-molecule systems [11]. These results indicate that Model #2 is robust, and that realistic values for its parameters can be determined by first-principles calculations. The impact of the orbital charging energy is, how-

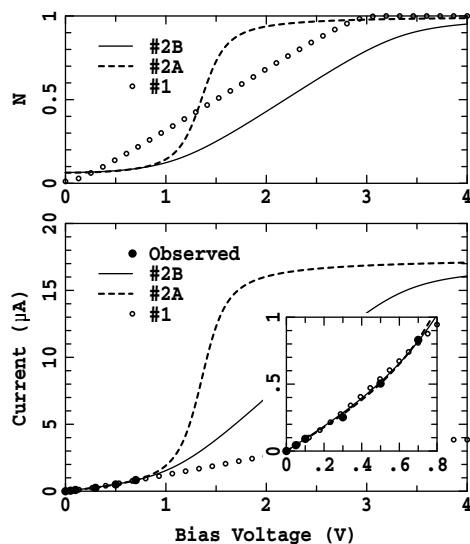


Fig. 3. The lower panel shows simulated I - V curves for 1,4-benzenedithiol chemisorbed between two gold contacts as calculated using Models #1, #2A, and #2B along with the experimental curve from Xiao et al. [26], while the upper panel shows the calculated molecular-orbital occupancy.

ever, only important for voltages at which significant charge transfer occurs. From each model, the predicted steady-state charge transfer to the molecule is also shown in Fig. 3, and the onset of significant charge transfer is readily correlated to the differences in the conductivities calculated for Models #2A and #2B. At low voltage, the current is dominated by electron tunnelling with little charge transfer to the molecule. All calculations using Model #2 have realistic boundary properties, avoiding the catastrophic failures that fully empirical models (e.g., power law or polynomial expansions) suffer outside of their parameterization range. However, significant differences are depicted in Fig. 3 between the results of Models #2A and #2B outside of their parameterization range, indicating that care must also be taken when using physically based models.

7. Conclusions

Two physically based models of a molecular component were developed and implemented in the general purpose circuit simulator *f*REEDA™ [20]. Of these, Model #1 was shown to be very useful in that it can be used as a functional form to interpolate experimental data; however it was found to be insufficiently robust to describe more complicated processes using physically meaningful parameters. Its extension, Model #2, was found to be robust, reproducing known analytical formulae describing the conduction through atomic wires, with first-principles DFT methods being applied to calculate its parameters with useful accuracy. Practical applications should, if possible, involve the optimization of the model parameters in order to obtain quantitative accuracy, which is limited due to the simplicity of the model, shortcomings in computational methods such as DFT, and the imprecisely known nature of the device interfaces.

A key aspect of this project is the generation of a circuit-element model that can be solved in realistic time in a complete circuit simulator involving potentially millions of different components. There is a trade off between simulation time and physical accuracy and we showed that the implemented models can be varied in their complexity to yield per component computation times ranging from 10 ms to 10 s. This flexibility constitutes a great asset in designing future molecular component based circuits.

Simpler alternatives to these physically based models can be readily generated using empirical representations ranging from limiting formulae such as Eq. (14) to polynomial or power-law expansions. While such approaches can be very computationally efficient and may include effects such as negative differential resistance and have been successfully applied in circuit simulators of entire devices [13–19], their parameters must be fitted to experimental data for each system of interest. Also, approaches such as power-law expansions have unphysical solutions outside of the parameterization range and must always be used

with caution. While physically based models typically have correct boundary properties, quantitative variations between feasible models can still be significant, as highlighted in Fig. 3, and hence fitting of the model parameters to experimental data remains the most reliable procedure for their usage. However, for new systems and for systems that are slight modifications of known ones, physically based approaches allow for useful models to be rapidly developed even when no direct electrical data are available to be fitted. This process could occur using *a priori* calculations of the molecular properties, as pursued herein, or using either known or easily measurable relationships between orbital energies and chemical substituent effects [53].

More complex alternatives to these models can be developed in which the entire component (the molecule and its connections) are simulated by first-principles quantum-mechanical methods, and indeed there is currently much research in this area. While such simulations may reach quantitative accuracy, their interpretation in terms of the key chemical properties influencing the molecular component will always be difficult to obtain. The construction of physically based models, however, involves an iterative process in which these key properties are built in and considered. For example, we modelled chemisorbed 1,4-benzenedithiol as if it were a gas-phase molecule interacting weakly with its environment. This may not be the most apt chemical model, with other alternatives including a weakly interacting thiolate and a weakly interacting excited-state species. While it is clear that the thiolate model is inappropriate [34], the excited-state model has not yet been properly investigated. If it were found to be apt, then the physical interpretation of the orbitals and quantities such as ϵ_0 in Model #2 would require modification, as would our basic understanding of molecular components *in situ*. The physically based models refined to include these and other effects will maintain the computational efficiency of the circuit simulator, allowing it to be applied to complex and multi-dimensional problems for which simple fitting of conductivity data are no longer feasible.

Acknowledgements

This material is based upon work supported in part by the Space and Naval Warfare Systems Center, San Diego under Grant No. N66001-01-1-8921 through North Carolina State University as part of the DARPA NeoCAD Program. This was also supported in part by contract N00014-01-1-0657 from DARPA/ONR, Grant CCR-0326157 from the National Science Foundation and from the Australian Research Council. The Center of Excellence for Computational Chemistry at the University of Ulm, Germany provided access to its supercomputing cluster for GAUSSIAN-03 calculations. This work has been made possible by the generous support of Alcatel Germany.

References

- [1] N.S. Hush, *J. Chem. Phys.* 28 (1958) 962.
- [2] N.S. Hush, *Prog. Inorg. Chem.* 8 (1967) 391.
- [3] R.A. Marcus, *J. Chem. Phys.* 24 (1956) 966.
- [4] A. Aviram, M.A. Ratner, *Chem. Phys. Lett.* 29 (1974) 277.
- [5] Y. Xue, S. Datta, M.A. Ratner, *J. Chem. Phys.* 115 (2001) 4292.
- [6] M. Brandbyge, J.-L. Mozos, P. Ordejon, J. Taylor, K. Stokbro, *Phys. Rev. B* 65 (2002) 165401-1.
- [7] G.K. Ramachandran, J.K. Tomfohr, J. Li, O.F. Sankey, X. Zarate, A. Primak, Y. Terazono, T.A. Moore, A.L. Moore, D. Gust, L.A. Nagahara, S.M. Lindsay, *J. Phys. Chem. B* 107 (2003) 6162.
- [8] P.S. Damle, A.W. Ghosh, S. Datta, *Phys. Rev. B* 64 (2001) 201403/1.
- [9] P. Damle, T. Rakshit, M. Paulsson, S. Datta, *Nanotechnol., IEEE Trans.* 1 (2002) 145.
- [10] K. Burke, R. Car, R. Gebauer, *Phys. Rev. Lett.* 94 (2005) 146803-1.
- [11] G.C. Solomon, J.R. Reimers, N.S. Hush, *J. Chem. Phys.* 122 (2005) 224502-1-7.
- [12] J.E. Ridley, M.C. Zerner, *Theor. Chim. Acta* 32 (1973) 111.
- [13] M.M. Ziegler, M.R. Stan, in: *Proceedings of the 2002 2nd IEEE Conference on Nanotechnology, 2002, IEEE-NANO 2002* (2002) 323.
- [14] M.R. Stan, P.D. Franzon, S.C. Goldstein, J.C. Lach, M.M. Ziegler, *Proc. IEEE* 91 (2003) 1940.
- [15] M.M. Ziegler, C.A. Picconatto, J.C. Ellenbogen, A. DeHon, D. Wang, Z. Zhong, C.M. Lieber, *Ann. NY Acad. Sci.* 1006 (2003) 312.
- [16] M.M. Ziegler, M.R. Stan, *IEEE Trans. Nanotechnol.* 2 (2003) 4.
- [17] C. Dwyer, M. Cheung, D. Sorin, *Proceedings of the 4th IEEE Conference on Nanotechnology* (2004) 386.
- [18] G. Snider, *Appl. Phys. A* 80 (2005) 1165.
- [19] S. Das, *Lect. Notes Phys.* 680 (2006), in press.
- [20] M. Steer, C. Christoffersen, N. Kriplani, et al, *fREEDA Circuit Simulator* (North Carolina State University, Raleigh, NC, USA). Available from: <http://www.freedda.org>.
- [21] D.P. Foty, *MOSFET modeling with SPICE: Principles and Practice*, Prentice Hall, 1997.
- [22] C.E. Christoffersen, U.A. Mughal, M.B. Steer, *Int. J. RF Microw. Comput. Eng.* 10 (2000) 164.
- [23] A. Griewank, D. Juedes, J. Utke, *Adol-C: A Package for the Automatic Differentiation of Algorithms Written in C/C++*, Tech. Univ. Dresden, Dresden, Germany, 1996, Version 1.7.
- [24] F. Zahid, M. Paulsson, S. Datta, in: H. Markoc (Ed.), *Advanced Semiconductors and Organic Nanotechniques*, Academic Press, New York, USA, 2003.
- [25] M. Paulsson, F. Zahid, S. Datta, in: S. Lyshevski (Ed.), *Handbook Of Nanotechnology*, CRC Press, Boca Raton, USA, 2003.
- [26] X. Xiao, B. Xu, N.J. Tao, *Nano Lett.* 4 (2004) 267.
- [27] M.A. Reed, C. Zhou, C.J. Muller, T.P. Burgin, J.M. Tour, *Science* 278 (1997) 252.
- [28] J.G. Kushmerick, D.B. Holt, J.C. Yang, J. Naciri, M.H. Moore, R. Shashidhar, *Phys. Rev. Lett.* 89 (2002) 086802.
- [29] J.G. Kushmerick, D.B. Holt, S.K. Pollack, M.A. Ratner, J.C. Yang, T.L. Schull, J. Naciri, M.H. Moore, R. Shashidhar, *J. Am. Chem. Soc.* 124 (2002) 10654.
- [30] J.G. Kushmerick, J. Naciri, J.C. Yang, R. Shashidhar, *Nano Lett.* 3 (2003) 897.
- [31] T. Dadosh, Y. Gordin, R. Krahne, I. Khivrich, D. Mahalu, V. Frydman, J. Sperling, A. Yacoby, I. Bar-Joseph, *Nature* 436 (2005) 677.
- [32] X.D. Cui, A. Primak, X. Zarate, J. Tomfohr, O.F. Sankey, A.L. Moore, T.A. Moore, D. Gust, G. Harris, S.M. Lindsay, *Science* (Washington, DC, United States) 294 (2001) 571.
- [33] M.A. Reed, *Proc. IEEE* 87 (1999) 652.
- [34] A. Bilić, J.R. Reimers, N.S. Hush, *J. Chem. Phys.* 122 (2005) 094708.
- [35] A.S. Duwez, *J. Electron. Spectrosc. Relat. Phenom.* 134 (2004) 523.
- [36] M.C. Bourg, A. Badia, R.B. Lennox, *J. Phys. Chem. B* 104 (2000) 6562.
- [37] W. Azzam, B.I. Wehner, R.A. Fischer, A. Terfort, C. Wöll, *Langmuir* 18 (2002) 7766.
- [38] J. Hubbard, *Proc. Roy. Soc. A* 240 (1957) 539.
- [39] S. Larsson, *Chem. Phys.* 326 (2006) 115.
- [40] J.G. Kushmerick, J. Lazorcik, C.H. Patterson, R. Shashidhar, D.S. Seferos, G.C. Bazan, *Nano Lett.* 4 (2004) 639.
- [41] W. Wang, T. Lee, I. Kretzschmar, M.A. Reed, *Nano Lett.* 4 (2004) 643.
- [42] L.E. Hall, J.R. Reimers, N.S. Hush, K. Silverbrook, *J. Chem. Phys.* 112 (2000) 1510.
- [43] B. Xu, N.J. Tao, *Science* 301 (2003) 1221.
- [44] B. Xu, X. Xiao, N.J. Tao, *J. Am. Chem. Soc.* 125 (2003) 16164.
- [45] R.H.M. Smit, C. Untiedt, G. Rubio-Bollinger, R.C. Segers, J.M. van Ruitenbeek, *Phys. Rev. Lett.* 91 (2003).
- [46] W. Tian, S. Datta, S. Hong, R. Reifenberger, J. Henderson, C.P. Kubiak, *J. Chem. Phys.* 109 (1998) 2874.
- [47] H. Bock, S. Mohmand, T. Hirabayashi, G. Maier, H.P. Reisenauer, *Chem. Ber.* 116 (1983) P273.
- [48] D.A. Armstrong, Q. Sun, G.N.R. Tripathi, R.H. Schuler, *J. Phys. Chem.* 97 (1993) 5611.
- [49] M.J. Frisch, G.W. Trucks, H.B. Schlegel, et al., *GAUSSIAN 03 Rev. B2*, Gaussian Inc., Pittsburgh, PA, 2003.
- [50] A.D. Becke, *J. Chem. Phys.* 98 (1993) 5648.
- [51] J.P. Perdew, Y. Wang, *Phys. Rev. B* 45 (1992) 13244.
- [52] W.J. Hehre, R. Ditchfield, J.A. Pople, *J. Chem. Phys.* 56 (1972) 2257.
- [53] R.A. Binstead, M.J. Crossley, N.S. Hush, *Inorg. Chem.* 30 (1991) 1259.
- [54] T. Hansen, T.B. Pedersen, K.V. Mikkelsen, *Chem. Phys. Lett.* 405 (2005) 118.